

Locational Dependence of Inertia's Impacts on Critical Clearing Time

Yijing Liu, *Student Member, IEEE*, Ti Xu, *Member, IEEE*, and Thomas J. Overbye, *Fellow, IEEE*

Department of Electrical and Computer Engineering

Texas A&M University

College Station, TX, USA 77843

Email: {yiji21, txu, overbye}@tamu.edu

Abstract—With the integration of renewable energy, system inertia may have a trend of decreasing in recent years, which increases the likelihood of transient instability. Inertia has impacts on voltage profiles and such impacts vary by location. After the system is subject to faults on buses or on transmission lines, bus voltages change differently as sum of inertia varies in sites that are either near or far away from violation locations. Critical clearing time (CCT) is a metric assessing condition of system stability. This paper displays how inertia changes affect CCT and how such impacts are location-dependent. An insightful preliminary study is carried out to reveal how inertia comes into play in bus voltage levels. Two case sets considering different oscillations are presented to verify inertia's locational impacts on CCT.

Index Terms—inertia, critical clearing time, locational impacts, transient stability, large-scale synthetic networks

I. INTRODUCTION

Resource inertia is a property that slows down the change of rotor speeds due to the existing power imbalance in electrical grid. Inertial response is provided by synchronous rotating masses and thus may decrease dramatically with the integration of large-scale light-weight gas turbines and renewable generation units [1]. According to previous work [2][3], integration of renewable energy results in system inertia's reduction, which may worsen post-fault frequency response. Transient stability is concerned with the ability of power system to return to stable condition and maintain synchronism, when the system is subjected to a severe disturbance, such as short-circuit faults on buses or transmission lines [4]. Voltage value is an important indicator that attests transient stability of power system. After the system is subject to some faults either within plants or on utility lines, voltage dips may occur and even cause transient instability from the system perspective of view [5]. To assist power system operators to obtain characteristics of the system transient stability, many metrics have been developed, one of which is called Critical Clearing Time (CCT) [6][7]. CCT is the maximum time when fault is cleared by some protection mechanisms and power system can still maintain its stability and synchronism. The goal of this paper is to study inertia's impacts on voltage stability in power system.

Sum of inertia in power system has impacts on system primary frequency responses and the system oscillation modes

[8][9]. Work done in [2] developed metrics for quantification of locational impacts of resource inertia on power system dynamic performances. Increasing world-wide wind power generator units brought new challenges to utilities and customers from power system voltage stability point of view [10–14]. Faults on transmission lines significantly disturb power system and cause dynamic voltage instability [15]. The proper use of realistic dynamic load models could capture physically accurate behavior in voltage recovery process after power system events [16]. Reference [17] provided a theoretical foundation for potential energy boundary surface method and [18] applied this method to obtain system CCT in several fault scenarios as the stability metric. This work is designed to reveal the relationship between system inertia and voltage levels. In particular, this paper studies how CCT changes as system inertia varies using large-scale network models. In particular, this paper focuses on inertia's locational effects on system critical clearing time .

This paper starts with simulations performed using the ACTIVSg200 [19] synthetic network to show how inertia affects bus voltages. Multiple stages after a fault is applied to the system are considered to provide more details about how inertia will affect system voltage levels. Based on simulation results from the preliminary study, this paper employs a 2000-bus case to investigate inertia's impacts on voltage using CCT as a performance metric. Variations in resource inertia with different electrical distances to fault and violation locations are implemented to show the locational dependence of inertia's impacts. What's more, one case set also includes poorly-damped oscillation modes. Large-scale synthetic network models in [19–23] are used in simulations throughout this paper.

Three more sections come as follows. In Section II, preliminary study is preformed to review how inertia affects bus voltages in power system. Simulation results using a large-scale case with varying inertia at different locations are provided in Section III to show location-dependent impacts of inertia, and Section IV provides conclusions of this paper and future work direction.

II. PRELIMINARY STUDIES

To reveal the relationship between system inertia and CCT after a fault is applied to the network, this section studies how

voltage differs in correspondence to inertia changes.

A. Case Description

This section uses the ACTIVSg200 case, which is available at [19]. This system is built on the footprint of Central Illinois. This case contains 49 generators with total system inertia of 159 s on a system base of 100 MVA. All generators are modeled with the GENROU machine model. All simulation results are obtained using the PowerWorld Simulator Version 20 [24]. The test case is subject to an event of a balanced 3-phase fault, which is applied to Bus 36 at 1s and the fault is cleared at 1.42s. Violations are defined when bus voltages fall below a limit value (i.e., 70% of pre-fault voltage [25]). The first violation is on the generator bus (No. 147), so we further explore the voltage profile at Bus 147 (Fig.1). To study inertia's effects on voltage levels, total system inertia is changed from 75% to 125% in increment of 5% and Fig. 1 shows different bus voltage profiles when inertia is changed. Five points are marked in the figure: A: time point right *before* the fault is applied to the system; B: time point right *after* the fault is applied to the system; C: time point right *before* the fault is cleared; D: time point right *after* the fault is cleared; E: first voltage dip *after* the fault clearing time. Near point B, the bus voltage profile obtained with 125% system inertia lies on the top and the profile with 75% system inertia lies at the bottom. As inertia is reduced, we observe lower minimum voltage after fault is cleared. There are 4 periods of interest ($A \rightarrow B$, $B \rightarrow C$, $C \rightarrow D$, $D \rightarrow E$) on each bus voltage profile. Fig. 2 shows bus voltage changes of period $B \rightarrow C$ under different inertia scenarios. Among 4 periods, period $B \rightarrow C$ has the most significant changes in $\Delta V_{B \rightarrow C}$ under different inertia scenarios. In the next subsection, we will focus on period $B \rightarrow C$. Another period of interest is $D \rightarrow E$, so we also go into this period in the following subsection.

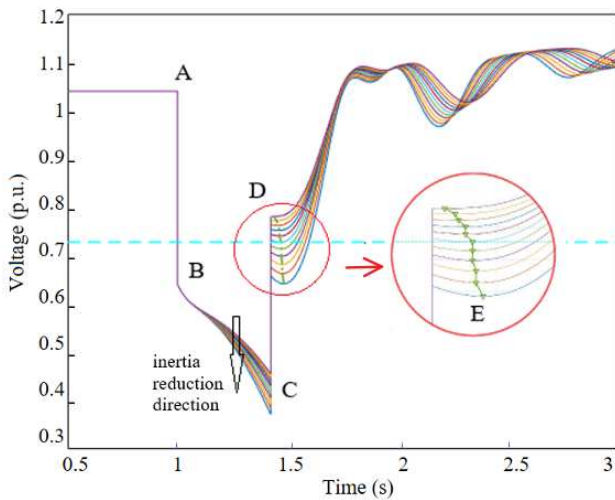


Fig. 1. Bus voltage profiles as inertia varies

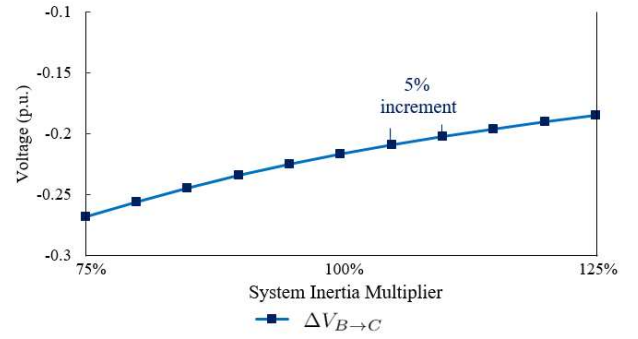


Fig. 2. $\Delta V_{B \rightarrow C}$ under different inertia scenarios

B. Voltage Dip During Fault

Bus voltages are computed using generator internal voltages and network electrical properties. In particular, the voltage level of each bus is more dependent on the generator that is (electrically) closest to that bus. Following analysis focuses on generator on Bus 147, whose internal voltage is calculated by three values $((1 + \omega), \psi_d'', \psi_q'')$. Fig.3 shows that ψ_d'' increases much more than other two values $((1 + \omega), \psi_q'')$ when inertia increases. In the GENROU model [26], increase in ψ_d'' value means either decrease in input I_d value or increase in another input E_{fd} . Trivial change in E_{fd} is seen during the fault period (in Fig.4), so increase in ψ_d'' is primarily the result of decreased I_d . Higher generator inertia results in lower generator internal current and then higher internal voltage. Further analysis will be provided to explain why a lower current is obtained when inertia is increased.

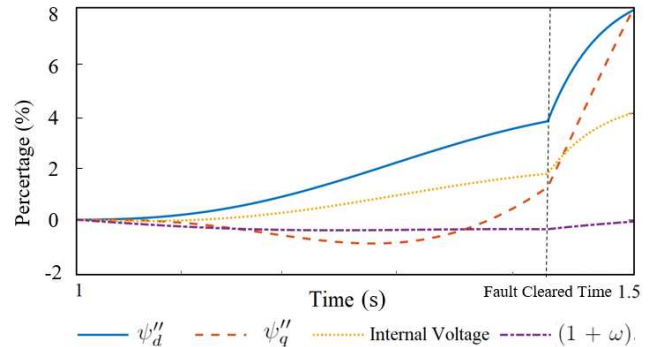


Fig. 3. Percentage changes in generator internal states between 75% and 125% system inertia

Both generator internal voltage and bus voltage are phasors with time-varying magnitudes and angles, which are affected by inertia changes. We compute $|\vec{E}_{Internal} - \vec{V}_{Bus}|$ in three cases. All cases have inertia changes from 75% to 125%. In case a, we only change inertia in generator 147; in case b, inertia in all generators but 147 is increased; in case c, inertia in all generators is increased. In scenario (1), we compute $|\vec{E}_{Internal} - \vec{V}_{Bus}|$ with 75% inertia in those selected generators; in scenario (2), inertia in those selected generators is

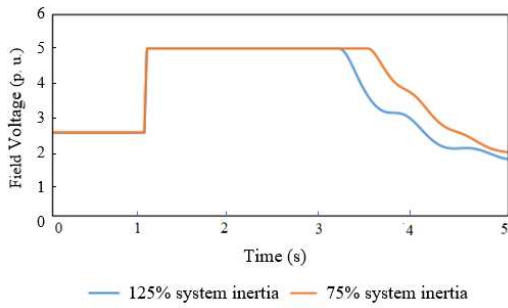


Fig. 4. E_{fd} values under different inertia values

increased to 125%; in scenario (3), inertia in those selected generators is still 125%, but angle differences of generator internal voltage and bus voltage are assumed to be the same as (1). In case a, as displayed in Fig.5 a, the computed $|\vec{E}_{Internal} - \vec{V}_{Bus}|$ in scenarios (1) and (2) are nearly the same while $|\vec{E}_{Internal} - \vec{V}_{Bus}|$ is significantly different in scenario (3). In case a, higher generator inertia results in slower rotor angle changes and smaller angle differences between generator internal voltage and bus voltage angle. $|\vec{E}_{Internal} - \vec{V}_{Bus}|$ becomes smaller, and smaller generator current is observed. In case b, higher inertia in all generators but 147 causes slower rotor angle changes in those selected generators. Bus 147 voltage angle becomes smaller. In addition, rotor angle change of Generator 147 is small, thus overall angle differences between Generator 147 internal voltage and Bus 147 voltage increase. The computed $|\vec{E}_{Internal} - \vec{V}_{Bus}|$ becomes larger, thus larger generator current is obtained. In case c, the overall effect is shown when system inertia increases. Increased inertia of generator 147 is dominant on changes of generator current, so a lower current is obtained when system inertia is increased. This subsection explains inertia's impacts on voltage and the next part will show how inertia changes affect system's CCT.

C. Post-Fault Minimum Voltage

After the fault is cleared, bus voltages increase instantly to the point D (period $C \rightarrow D$), but may drop to a lower value point E (period $D \rightarrow E$) (in Fig. 2). That's because generator internal current increases (as demonstrated in Fig. 6) as soon as the fault is cleared and generator internal voltage drops due to the similar process as discussed in Subsection B. Displayed in Fig.2, when the fault is applied at 1s and cleared at 1.4229s, the minimum voltage point E lies on the pre-defined criterion (i.e., 70% of pre-fault voltage value [25]), so current clearing time (0.4229s) is the critical clearing time (CCT) of the system. When the system has further decrease in inertia, voltage level is worse than before, so a lower post-fault nadir point E is observed. The previous fault duration (0.4229s) is longer than fault duration that the modified system can have without violation occurring in the inertia-reduced system. As a result, the modified system CCT is smaller compared to original (100% inertia) system. As such, inertia has impacts on CCT.

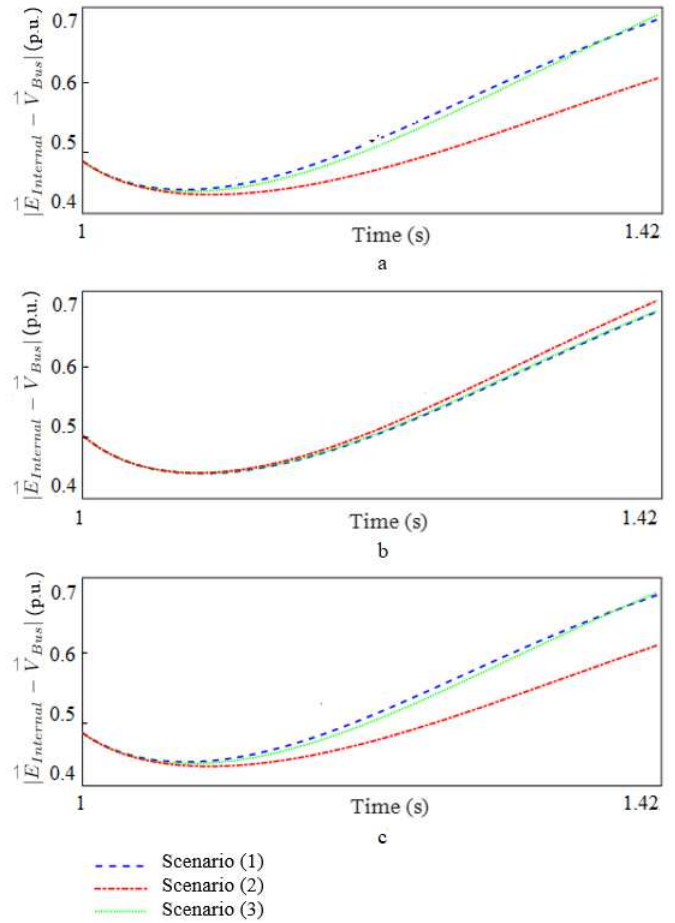


Fig. 5. $|\vec{E}_{Internal} - \vec{V}_{Bus}|$ in three different cases

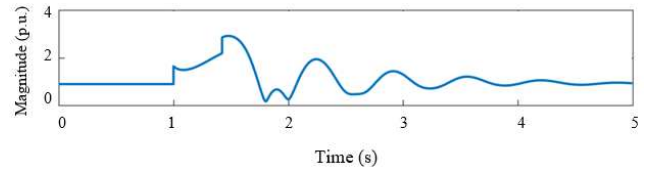


Fig. 6. Generator Internal Current

III. ILLUSTRATIVE SIMULATION RESULTS

This paper illustrates inertia's location-dependent impacts on system CCT using a synthetic 2000-bus network model - ACTIVSg2000 [19]. As shown in Fig. 7, this model is built on the Electric Reliability Council of Texas (ERCOT) footprint. This is a synthetic power system model that does not represent the actual grid, but the model is designed to be statistically and functionally similar to actual electric grids. Eight areas are defined in this model. Multiple machine/governor/exciter/stabilizer models for each fuel type are included in this case. Online generators have total system inertia of 3814.18 s using system base of 100 MVA. Two cases (with either well damped or poorly damped oscillation) are considered in simulations.

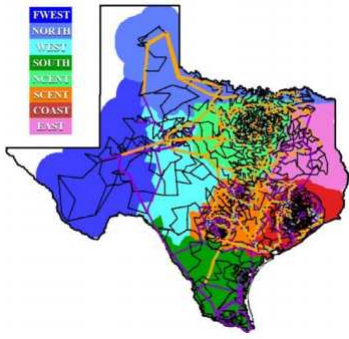


Fig. 7. One-line diagram of the 2000-bus case [2]

A. Case Set I - with well damped oscillation

Case Set I has a balanced 3-phase fault applied to Bus 6003. Three types of violations are considered (details in Table I). Violations occur when bus voltages fall below a limit value for a time longer or equal to limit duration [25]. The first violation occurs on a generator bus in the same area (i.e., Bus 6009). This case set aims to study how CCT is affected by near and far away inertia changes. We increase inertia of selected generators (instead of all 68 generators) in different parts of the system and perform same simulations to obtain CCT under different ratios¹. In this case set, all violations occur in the same area. Table.II provides details on Case Set I.

TABLE I
CONSIDERED VIOLATIONS DETAILS

Type	Limit Value	Limit Duration
Voltage Dip Load Bus	-25%	0
Voltage Dip Non-load Bus	-30%	0
Voltage Dip Load Bus Duration	-20%	0.333 (s)

Fig.8 displays CCT changes with respect to inertia changes in selected generators (all selected generators in Cases I.1 and I.2, the faulted bus and the violation bus are in the same area). In Case I.1, when inertia increases, CCT in each subset increases as well. We note that increasing inertia in electrically nearest 11 generators (instead of all 68 generators) has nearly the same effect in increasing CCT. In general, when fewer generators are selected, smaller CCT is observed under each ratio. In Case I.2, increasing inertia in modified selected generators does not obviously affect CCT. Significant reduction in CCT is observed when the generator at violation location is excluded from inertia increases. Generally when more generators are excluded from inertia increases, smaller CCT is obtained under each ratio. In Case I.3, no obvious change in CCT when inertia increases are in generators located

¹We increases inertia in this area (originally 760.55 s) & All areas except this area (originally 3053.63 s) by 0 s all the way up to 500 s in increment of 100 s. The corresponding ratio is from 1 to $(760.55 + 500)/760.55 \approx 1.65$ (in this area) & from 1 to $(3053.63 + 500)/3053.63 \approx 1.16$ (outside this area).

TABLE II
DETAILS ON CASE SET I

Case I.1	
Subset	Selected Generators
1.a	All in this area
1.b	The one at violation location
1.c	Electrically nearest 5 (around violation location)
1.d	Electrically nearest 11 (around violation location)
Case I.2	
Subset	Selected Generators
2.a	All in this area
2.b	Except the one at violation location
2.c	Except electrically nearest 5 (around violation location)
2.d	Except electrically nearest 11 (around violation location)
Case I.3	
Subset	Selected Generators
3.a	All generators except those located in this area

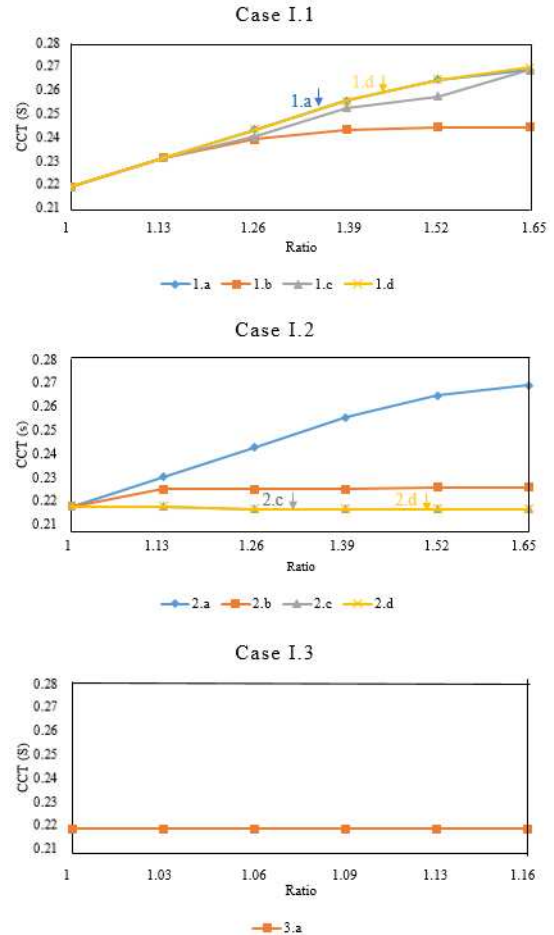


Fig. 8. Multiple CCTs under different inertia scenarios in case set I

outside this area. For now, it's clear that inertia's impacts are more significant in locations that are electrically close to violation location. Inertia changes in electrically nearest (i.e., around violation location) generators have greater impacts on CCT.

B. Case Set II - with poorly damped oscillation

In Case Set II, several subsets (i.e., II.a ~ II.j) are performed to reveal how inertia changes affect CCT in a system with poorly damped oscillation. All subset details are shown in Table.IV and will be clearly explained in the following part.

After a balanced 3-phase fault is applied to Bus 7037 at 1s and cleared at 1.140s, the first violation (i.e., voltage dip load bus duration violation) occurs in Area 1 on Bus 1058 (II.a). In II.b, inertia reduction is performed in the violation location of II.a (Area 1) and the previous violation vanishes. Since sum of inertia in Area 1 is small (i.e., 83.76 s), we only reduce inertia in Area 1 by 50 s. When the same fault is applied to the same bus but we clear it after a longer period (i.e., 0.307s), another violation appears in Area 8 on Bus 8005 (i.e., II.c) and the previous violation does not occur. In II.d, we reduce inertia in Area 1 by 50 s and clear the fault at 1.307s. The violation occurs in Area 8. Table.III summarizes simulation details up to now. For comparison, we perform inertia reduction in six more subsets and divide them into two groups: II.e & II.g & II.i (fault clear time is 1.140s), II.f & II.h & II.j (fault clear time is 1.307s). Respectively, inertia reduction area is Area 8 (violation location of II.c & II.d) in subsets II.e and II.f, Area 7 (fault location) in subsets II.g and II.h, and Area 5 (an area, which is neither a fault location nor a violation location) in subsets II.i and II.j.

TABLE III
DETAILS OF FOUR SUBSETS AND CORRESPONDING CLEAR TIME

	II.a	II.b	II.c	II.d
Violation Location	Bus 1058	No	Bus 8005	Bus 8005
Clear Time (s)	1.140	1.140	1.307	1.307

TABLE IV
CASE DETAIL AND CORRESPONDING CLEAR TIME

	Clear Time (s)	Subset Detail	Violation Location
II.a	1.140	0 s (Area 1)	Area 1
II.b	1.140	-50 s (Area 1)	No violation
II.c	1.307	0 s (Area 1)	Area 8
II.d	1.307	-50 s (Area 1)	Area 8
II.e	1.140	-50 s (Area 8)	Area 1
II.g	1.140	-50 s (Area 7)	Area 1
II.i	1.140	-50 s (Area 5)	Area 1
II.f	1.307	-50 s (Area 8)	Area 8
II.h	1.307	-50 s (Area 7)	Area 8
II.j	1.307	-50 s (Area 5)	Area 8

Table.IV provides details of all subsets in Case Set II. Fig.9 shows that bus voltage profiles either vary in time differently in some subsets (e.g., II.a & II.d) or behave similarly in other subsets (e.g., II.a & II.e & II.g & II.i; II.c & II.f & II.h & II.j). In II.a, Bus 1058's voltage falls below the limit (i.e., 80% of pre-fault voltage) for a time longer than limit duration (i.e., 0.333s), so the first violation occurs; there is no violation on Bus 8005 now. In II.d, Bus 1058's voltage does not violate while Bus 8005 has a 'load bus duration violation'. In II.b,

there is no violation in the system; in II.c, the first violation occurs on Bus 8005. Compared to II.a, inertia changes does not significantly affect voltage profiles in II.e & II.g & II.i. Similarly, voltage profiles of II.f & II.h & II.j are reasonably close to II.c's voltage profile.

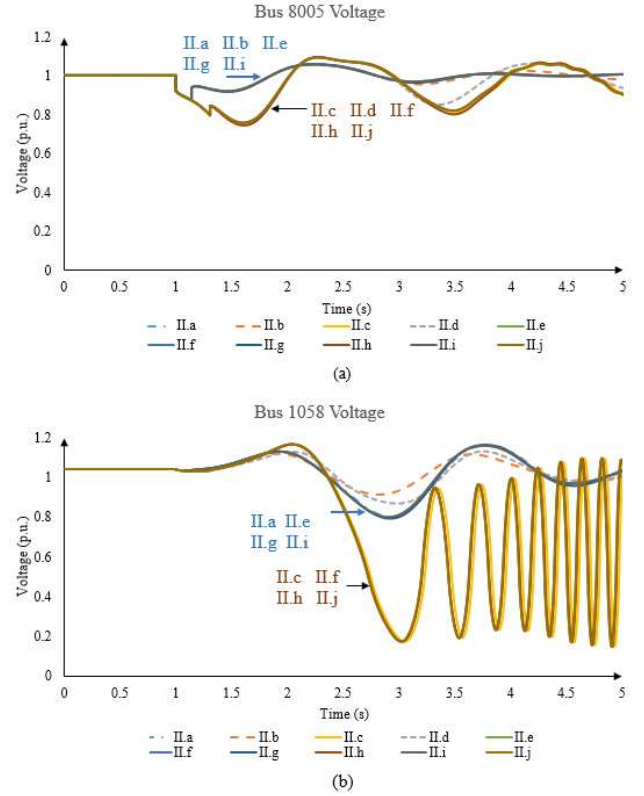


Fig. 9. Bus voltage magnitude plot of violation buses

Inertia reduction in Area 1 does not affect voltage profile of Bus 8005, but magnitude of Bus 1058 has changed a lot (II.a & II.b). Results in [8] indicating that inertia has large effects on local oscillations, inertia reduction may deteriorate or alleviate oscillations, thus bus voltages change in Area 1 when we reduce inertia in Area 1 (i.e., II.a & II.b; II.c & II.d in Bus 1058 voltage profile). Shown in Fig.9, violation in Area 1 vanishes when 50 s inertia reduction is applied in Area 1 (i.e., II.a & II.b). All subsets show that local inertia reduction play an important role of local voltage level, but do not have vital impacts on global voltages. In comparison subsets (i.e., II.a & II.e & II.g & II.i; II.c & II.f & II.h & II.j), remote inertia reductions have trivial effects on local voltages and thus CCT do not vary much. Till this moment here, inertia's locational impacts on bus voltages are clearly revealed, and such effects are local but rather than global.

Simulation results in this section demonstrate inertia's location-dependent impacts on bus voltages. The locational impacts of inertia play the most significant role when inertia changes are applied near voltage violation locations.

IV. CONCLUSIONS

In this paper, two synthetic network models were used to show inertia's locational impacts on CCT. The ACTIVSg2000 synthetic network was used to study how inertia affects bus voltages and why inertia plays an important role in maintaining a longer CCT. The ACTIVSg2000 synthetic network was applied to display that inertia changes had location-dependent impacts on bus voltages. Generally, effects of inertia changes are local, rather than global. In addition, inertia had the most significant impacts when inertia changes are electrically near to violation locations.

Only voltage violation type is considered when we obtain CCT and more work need to be done with frequency violation type. It is also of interest to consider multiple faults in simulations. We will include these studies in future work.

ACKNOWLEDGEMENT

This work was supported by the U.S. Department of Energy Consortium of Electric Reliability Technology Solutions (CERTS).

REFERENCES

- [1] R. G. De Almeida and J. P. Lopes, "Participation of doubly fed induction wind generators in system frequency regulation," *IEEE transactions on power systems*, vol. 22, no. 3, pp. 944–950, 2007.
- [2] T. Xu, Y. Liu, and T. J. Overbye, "Metric development for evaluating inertia's locational impacts on system primary frequency response," in *Texas Power and Energy Conference (TPEC), 2018 IEEE*, 2018, pp. 1–6.
- [3] I. Erlich, K. Rensch, and F. Shewarega, "Impact of large wind power generation on frequency stability," in *Power Engineering Society General Meeting, 2006. IEEE*, 2006, pp. 8–pp.
- [4] P. Kundur, J. Paserba, V. Ajjarapu, G. Andersson, A. Bose, C. Canizares, N. Hatziairgiou, D. Hill, A. Stankovic, C. Taylor *et al.*, "Definition and classification of power system stability IEEE/Cigre joint task force on stability terms and definitions," *IEEE transactions on Power Systems*, vol. 19, no. 3, pp. 1387–1401, 2004.
- [5] L. Conrad, K. Little, and C. Grigg, "Predicting and preventing problems associated with remote fault-clearing voltage dips," *IEEE Transactions on industry applications*, vol. 27, no. 1, pp. 167–172, 1991.
- [6] L. G. Roberts, A. R. Champneys, K. R. Bell, and M. di Bernardo, "Analytical approximations of critical clearing time for parametric analysis of power system transient stability," *IEEE Journal on Emerging and Selected Topics in Circuits and Systems*, vol. 5, no. 3, pp. 465–476, 2015.
- [7] Z. Eleschova, M. Smitkova, and A. Belan, "Evaluation of power system transient stability and definition of the basic criterion," *International journal of energy*, vol. 4, no. 1, pp. 9–16, 2010.
- [8] T. Xu, W. Jang, and T. J. Overbye, "Location-dependent impacts of resource inertia on power system oscillations," in *Proceedings of the 51st Hawaii International Conference on System Sciences*, 2018.
- [9] D. Wu, M. Javadi, and J. N. Jiang, "A preliminary study of impact of reduced system inertia in a low-carbon power system," *Journal of Modern Power Systems and Clean Energy*, vol. 3, no. 1, pp. 82–92, 2015.
- [10] F. Zhou, G. Joos, and C. Abbey, "Voltage stability in weak connection wind farms," in *Power Engineering Society General Meeting, 2005. IEEE*, pp. 1483–1488.
- [11] R. R. Londero, C. de Mattos Affonso, and J. P. A. Vieira, "Long-term voltage stability analysis of variable speed wind generators," *IEEE Transactions on Power Systems*, vol. 30, no. 1, pp. 439–447, 2015.
- [12] L. Meegahapola and T. Littler, "Characterisation of large disturbance rotor angle and voltage stability in interconnected power networks with distributed wind generation," *IET Renewable Power Generation*, vol. 9, no. 3, pp. 272–283, 2014.
- [13] M. P. Palsson, T. Toftevaag, K. Uhlen, and J. O. G. Tande, "Large-scale wind power integration and voltage stability limits in regional networks," in *Power Engineering Society Summer Meeting, 2002 IEEE*, vol. 2. IEEE, 2002, pp. 762–769.
- [14] M. J. Hossain, H. R. Pota, M. A. Mahmud, and R. A. Ramos, "Investigation of the impacts of large-scale wind power penetration on the angle and voltage stability of power systems," *IEEE Systems journal*, vol. 6, no. 1, pp. 76–84, 2012.
- [15] M. A. Yalcin, "The effects of faults on voltage stability of long electrical power transmission systems," in *Electrotechnical Conference, 1998. MELECON 98., 9th Mediterranean*, vol. 2. IEEE, 1998, pp. 1093–1097.
- [16] D. J. Hill, "Nonlinear dynamic load models with recovery for voltage stability studies," *IEEE transactions on power systems*, vol. 8, no. 1, pp. 166–176, 1993.
- [17] H.-D. Chiang, F. F. Wu, and P. P. Varaiya, "Foundations of the potential energy boundary surface method for power system transient stability analysis," *IEEE Transactions on circuits and systems*, vol. 35, no. 6, pp. 712–728, 1988.
- [18] P. K. Naik, N.-K. C. Nair, and A. K. Swain, "Impact of reduced inertia on transient stability of networks with asynchronous generation," *International Transactions on Electrical Energy Systems*, vol. 26, no. 1, pp. 175–191, 2016.
- [19] "Electric Grid Test Case Repository". [Online]. Available: <https://electricgrids.engr.tamu.edu/>
- [20] T. Xu, A. B. Birchfield, K. S. Shetye, and T. J. Overbye, "Creation of synthetic electric grid models for transient stability studies," in *The 10th Bulk Power Systems Dynamics and Control Symposium (IREP 2017)*, 2017.
- [21] T. Xu, A. B. Birchfield, and T. J. Overbye, "Modeling, tuning and validating system dynamics in synthetic electric grids," *IEEE Transactions on Power Systems*, 2018.
- [22] A. B. Birchfield, K. M. Gegner, T. Xu, K. S. Shetye, and T. J. Overbye, "Statistical considerations in the creation of realistic synthetic power grids for geomagnetic disturbance studies," *IEEE Transactions on Power Systems*, vol. 32, no. 2, pp. 1502–1510, 2017.
- [23] A. B. Birchfield, T. Xu, K. M. Gegner, K. S. Shetye, and T. J. Overbye, "Grid structural characteristics as validation criteria for synthetic networks," *IEEE Transactions on power systems*, vol. 32, no. 4, pp. 3258–3265, 2017.
- [24] "PowerWorld". [Online]. Available: <https://www.powerworld.com/>
- [25] "Voltage and Reactive Control". [Online]. Available: <https://www.nerc.com/files/BAL-002-WECC-2.pdf>
- [26] P. Sauer and M. Pai, *Power System Dynamics and Stability*. Stipes Publishing L.L.C., 2006.